Astron. Astrophys. 315, L173–L176 (1996)

ASTRONOMY
AND
ASTROPHYSICS

Detection of hot, abundant water toward AFGL 2591⋆

F.P. Helmich[1], E.F. van Dishoeck[1], J.H. Black[2], Th. de Graauw[3], D.A. Beintema[3,4], A.M. Heras[4], F. Lahuis[4], P.W. Morris[4,5], and E.A. Valentijn[3,4]

[1] Leiden Observatory, P.O.-Box 9513, 2300 RA Leiden, The Netherlands
[2] Onsala Space Observatory, Chalmers University of Technology, S-439 92 Onsala, Sweden
[3] SRON, P.O.-Box 800, 9700 AV Groningen, The Netherlands
[4] ISO Science Operation Center, Astrophysics Division of ESA, P.O.-Box 50727, E-28080 Villafranca/Madrid, Spain
[5] SRON, Sorbonnelaan 2, 3584 CA Utrecht, The Netherlands

Received 1 July 1996 / Accepted 21 August 1996

Abstract. We present the first detection of absorption lines within the bending vibration of water in the interstellar medium using the ISO–SWS. More than 30 lines between 5.5 and 6.6 μm are detected toward the bright infrared source GL 2591, which arise most likely in the dense molecular cloud core surrounding the young stellar object. Comparison with model spectra indicates a high excitation temperature ($T_{\rm ex} > 200$ K) and a high abundance $[H_2O]/[H_2] \sim (2-6)\,10^{-5}$. We speculate on the origin of the hot water, and the consequences for the chemistry.

Key words: ISM: abundances – ISM: molecules – ISM: clouds – ISM: individual: AFGL 2591

1. Introduction

Due to the large amount of water vapour in the Earth's atmosphere, water has been been an extremely difficult molecule to detect in interstellar space. Starting with Cheung et al. (1969), maser lines at radio wavelengths were long considered to be the only sign-posts of (non–thermal) water. Advancements in infrared instrumentation and the availability of the Kuiper Airborne Observatory (KAO) resulted in a $2-5\sigma$ detection of water toward Orion through its ν_3 ro-vibrational band by Knacke et al. (1988) and Knacke & Larson (1991). At sub–millimeter wavelengths ground–based, air– and balloon–borne observations of $H_2^{16}O$ and $H_2^{18}O$ lines have been used to infer the presence of water and obtain an estimate of its abundance (e.g., Waters et al. 1980; Phillips et al. 1980; Wannier et al. 1991; Jacq et al. 1988; Cernicharo et al. 1990, 1994; Gensheimer et al. 1996; Zmuidzinas et al. 1996; Tauber et al. 1996). These observations are hampered by the fact that usually only a single line is observed, which is insufficient to constrain the excitation. Also, the lines are seen in emission in large beams, ranging from $> 10''$ for ground-based telescopes up to arcminutes for airborne observatories.

The *Short Wavelength Spectrometer* (SWS) (de Graauw et al., 1996) on board the *Infrared Space Observatory* (ISO, Kessler et al., 1996) provides an unique opportunity to study the ro–vibrational fundamental bands of water in absorption against bright infrared continuum sources. In contrast with the emission data, only a pencil beam to the infrared source is probed, which minimizes the complications due to the small–scale physical and chemical heterogeneity of star–forming regions, as revealed by millimeter interferometers (e.g., Blake et al. 1996). Because lines from all rotational levels are present within a vibrational band, the complete spectrum yields a direct estimate of the level populations along the line of sight. The main limitation of ISO is its spectral resolving power, $\lambda/\Delta\lambda \approx 1350$ at 6 μm, since the lines are intrinsically much narrower. This limits the sensitivity so that only high column densities can be detected and complicates the interpretation because detectable lines will often be saturated.

GL 2591 has been a popular target at near– and mid–infrared wavelengths, following the discovery of strong gas-phase infrared absorption lines of CO by Lacy et al. (1984). High resolution ground–based spectroscopic data of CO and ^{13}CO by Geballe & Wade (1985) and Mitchell et al. (1989, 1990), and of C_2H_2 and HCN by Carr et al. (1995), have revealed several components along the line of sight, containing both cold gas with narrow lines, and warm gas with broad lines up to 130 km s^{-1}. The total column density in CO is large, $> 10^{19}$ cm^{-2}. The ISO observations are particularly sensitive to the warm, broad–line component.

Send offprint requests to: F.P. Helmich

⋆ Based on observations with ISO, an ESA project with instruments funded by ESA Member States (especially the PI countries: France, Germany, the Netherlands and the United Kingdom) and with the participation of ISAS and NASA

2. Observations and reduction

Water has three infrared–active vibrational modes. The ν_2 bending mode at 6 μm was chosen for observations, because it has the largest oscillator strength and contains lines which are well shifted from the water ice band. Also, the infrared continuum of the embedded young stellar objects is much stronger at 6 μm than around 2.7 μm, where the symmetric and asymmetric stretch occur.

The observations of GL 2591 were performed during the ISO Performance Verification Phase in revolution 28 (December 15, 1995). The measurements consist of SWS AOT06 observations of a small, selected wavelength range between 5.68 and 6.63 μm. The resolving power of the spectrometer is 1350 at 6 μm and changes only slightly over the observed range. The aperture is $14'' \times 20''$ in this setting and observations are diffraction limited. A single infrared source, GL 2591 IRS1, dominates the infrared continuum emission, although many weak infrared sources surrounding IRS1 are present in the beam. Since GL 2591 is very bright, $\sim$ 300 Jy at 6 μm, the shortest integration time per grating setting was sufficient, resulting in a total integration time of about 10 minutes.

Data reduction was performed in the standard mode. Comparison with both PHOT-S and ground-based data by the SIDT (SWS Instrument Dedicated Team) suggests that the photometric calibration is within 20% (Schaeidt et al. 1996). Note that this uncertainty does not affect our results, since only the relative absorption is used in the analysis.

As a last step, the data are rebinned on a grid with a constant spacing in wavelength. A spectral resolution of 1350 was used with an oversampling of 3. The spectral resolution was determined from unresolved lines in other observing programs (Valentijn et al. 1996). The final spectrum has a S/N on the continuum of $\sim$40.

3. The model water spectrum

Figure 1 shows the resulting ISO–SWS spectrum of GL 2591 in the 5.68–6.63 μm range. Many features are seen, which absorb 5–15% of the continuum and are significant at the 2–6σ level. The true noise in the spectum is best seen in the 6.25–6.30 μm region. Virtually all of the features can be ascribed to H_2O absorption lines in the ν_2 bending mode. The position of lines originating from the lowest 0_{00}, 1_{01}, 1_{10} and 1_{11} H_2O levels are indicated by tickmarks in the spectrum, and coincide with the strongest features in the spectrum. In total, at least 20 lines due to ortho–H_2O and 14 lines to para–H_2O can be identified. No lines of $H_2^{18}O$ or vibrationally–excited H_2O are seen.

Due to the fact that water is a non–linear molecule, its rotational energy level structure is very complex. This is reflected directly in the ro-vibrational spectrum, which is very different from the regular spectrum of a linear molecule such as CO (see van Dishoeck et al. 1996). This makes it difficult to analyze the measured spectrum without a detailed model. Here we follow the approach taken in Helmich (1996) to obtain simulated spectra. The necessary molecular data such as oscillator strengths and line positions were taken from the HITRAN data base (Rothman et al. 1992), but were checked against the measurements of Camy–Peyret & Flaud (1976).

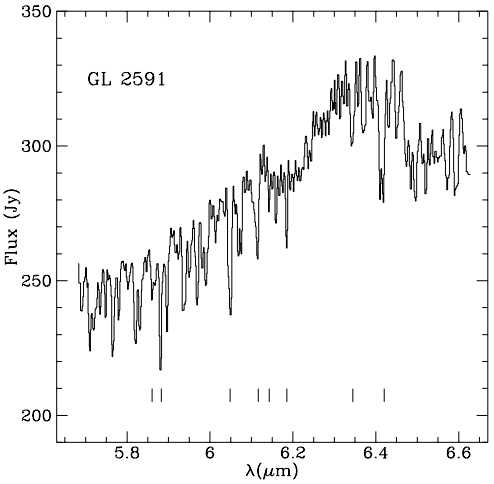

Fig. 1. ISO–SWS spectrum of GL 2591 (Coordinates (B1950.0): 20^h 27^m $35\overset{s}{.}8$ $+40°01'14.0''$). The multitude of water absorption lines is clearly visible. The broad absorption features at 6.2 and 6.5 μm may be due to other gas– or solid state features (see text).

In the simplest model, it is assumed that the water level populations can be characterized by a single excitation temperature, which should be close to the kinetic temperature if LTE conditions exist. This allows calculation of the column density N_j in each level for a given total column density. The spectrum is then obtained using a Voigt profile $\phi(\lambda - \lambda_0)$ for each line. The Doppler parameter $b_{\rm D}$ is related to the full width half maximum through $b_{\rm D} = \Delta v/2\sqrt{\ln 2}$. The optical depth can be expressed as: $\tau(\lambda) \sim \sum_j N_j f_j \phi(\lambda - \lambda_0)$. Optical depths are converted to relative intensity through $y = e^{-\tau}$. Finally, the spectrum is convolved with a gaussian function of width equal to the instrumental resolution. Models were run for different combinations of excitation temperature, Doppler parameter and column density.

4. Analysis

4.1. H_2O excitation

Figure 2 shows the normalized ISO–SWS spectrum toward GL 2591, compared with model spectra for three different excitation temperatures. The best fit to the data is obtained using $T_{\rm ex} \approx 300$ K. The low temperature model clearly has fewer water lines than observed. The features around 5.718, 5.897 and 5.968 μm arising from lower levels 4_{13} (396 K), 4_{14} (324 K) and 3_{13} (205 K) are particularly revealing in this respect. The 1000 K model has enough lines, but their relative strengths do not compare well with the observed spectrum. Note that the strength of observed features above 6.4 μm is less reliable due to the uncertain placement of the continuum (see Figure 1). The origin of the dip around 6.5 μm is unclear, but it coincides with

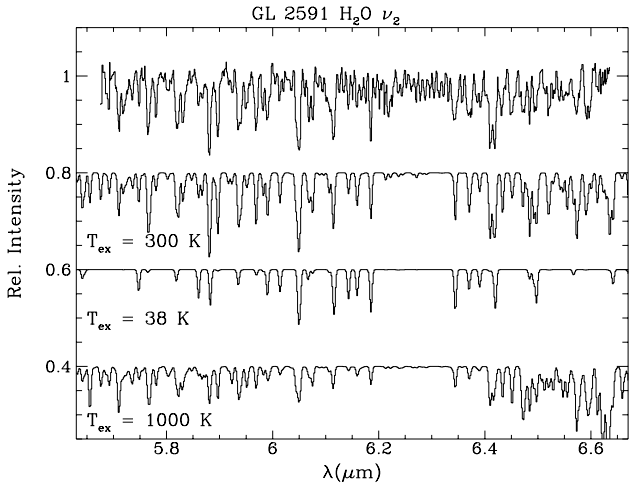

Fig. 2. From top to bottom: Normalized ISO–SWS spectrum observed toward GL 2591; theoretical spectra with T_{ex} = 300 K, b_D = 7.5 km s^{-1}; T_{ex} = 38 K, b_D = 5.3 km s^{-1}; and T_{ex} = 1000 K, b_D = 7.8 km s^{-1}, shifted by -0.2, -0.4, and -0.6 respectively. All model spectra have $N(H_2O) = 2.\ 10^{18}$ cm^{-2}.

the position of the ν_3 band of CS_2. No plausible identification of the dip around 6.2 μm has yet been found.

The high excitation temperature of water of 300 K is confirmed by a crude rotation diagram. Here the lines are assumed to be optically thin, and their depth to be representative of the equivalent widths (i.e., constant line width). Although the S/N of the data is limited, multiple lines out of the same lower level are observed, so that the resulting populations are more reliable. For both ortho– and para–water an excitation temperature of $250 - 400$ K is found.

The temperatures chosen in the model spectra in Figure 2 correspond to the temperature components found in the CO observations of Mitchell et al. (1989, 1990). Those data were of much higher spectral resolution than the present ISO results. Mitchell et al. derive three different velocity and temperature components from the ^{13}CO lines: (i) a cold component with T=38 K and $b_D \approx 5.3$ km s^{-1}; (ii) hot gas with T=1000 K, $b_D \approx 7.7$ km s^{-1} at virtually the same velocity; and (iii) warm gas with T=200 K and $b_D \approx 7.5$ km s^{-1}, shifted by –20 km s^{-1} in velocity. These three components have comparable column densities of ^{13}CO of 10^{17} cm^{-2}. In addition, a much smaller amount of warm, blue–shifted gas with more than 100 km s^{-1} line width and $T \approx 500$ K is seen. None of these components can be distinguished at the resolution of the ISO data. Carr et al. (1995) observed C_2H_2 and HCN infrared absorption, and found the two species present in both warm and hot components, but not in the cold gas. Their average excitation temperature is 300–400 K, similar to that found here for H_2O. Thus, it is likely that the H_2O originates in the same warm and hot components.

The fact that the deviation from a uniform H_2O excitation temperature of 300 K is not large places constraints on the excitation conditions. The strong rotational transitions of water in the far-infrared and the ν_2 vibrational transitions near 6 μm couple its rotational levels readily to the radiation field. In order for collisional processes to compete with radiative processes, the density must be very high, $n(H_2) \approx 10^9$ cm^{-3} or more. Consider the processes that affect the population of the 2_{21} level: spontaneous transitions to lower states occur with a summed rate of 0.29 s^{-1}, while the collisionally induced transitions out of this level have a summed rate $\sim 2 \times 10^{-10} n(H_2)$ at T = 300 K, based on the He–H_2O collision rates of Green et al. (1993) scaled by a factor of 1.5 for H_2. The near–infrared continuum of GL 2591 around 6 μm can be fit with a dust temperature of 300–350 K, whereas the far–infrared emission at 50-300 μm is consistent with a lower dust temperature of 40–100 K and a total extinction of a few hundred magnitudes. Continuum radiation with a brightness temperature of 300 K at 6 μm will induce absorptions out of 2_{21} at a rate of 7×10^{-3}, while radiation with an even lower brightness temperature of 40–100 K at wavelengths 50–200 μm will induce both absorptions and emissions at a total rate of 0.023 to 0.35 s^{-1}. Thus the observed high rotational excitation could be achieved either by collisions in 300 K gas at very high density, $n(H_2) \geq 10^9$ cm^{-3}, or by radiative excitation in a less dense region of dust with the observed range of color temperatures. At the densities $n(H_2) \approx 3 \times 10^7$ cm^{-3} inferred from the analyses of HCN and C_2H_2 (Carr et al. 1995) and of ^{13}CO (Mitchell et al. 1989), a mixture of radiative and collisional processes must almost certainly be at work here. In order to assess the role of H_2O as a coolant, these radiative and collisional contributions must be better understood.

The complicated excitation of H_2O (e.g. Neufeld & Melnick 1991) permits strong maser action at 22 GHz and weaker amplification in submillimeter transitions (Melnick et al. 1993). In our spectra, weak lines arising out of levels as high as 6_{16}, the upper state of the 22 GHz maser line, may be visible, but data of higher S/N are needed to confirm this. Resolved absorption line data would constrain maser models and help determine whether the masers are radiatively or collisionally pumped. Maser emission at 22 GHz has been observed toward GL 2591 most recently by Tofani et al. (1995).

4.2. H_2O abundance and chemistry

For a given value of b_D, the depth of the absorption is directly related to the column density, even in the optically thick case. For T_{ex}=300 K and b_D = 7.5 km s^{-1}, $N(H_2O) = 2.\ 10^{18}$ cm^{-2} provides the best fit to the observed spectrum. Because so many lines are detected with different intrinsic line strengths and optical depths, the uncertainty in this value is less than a factor of two. Different b_D values between 5 and 12 km s^{-1} also do not change the results by more than 50%.

It is difficult to put limits on the amount of H_2O in the cold and hot components. Because the lines out of the lowest levels are somewhat optically thick, a H_2O column density up to $5.\ 10^{17}$ cm^{-2} could be hidden in the cold component for b_D = 5.3 km s^{-1}. The best determination of the relative amount of H_2O in the hot 1000 K gas will come from observations outside the wavelength range observed here. Such observations are planned but have not yet been taken.

The ^{13}CO column density for the 200 K component found by Mitchell et al. (1989) of $1.1\ 10^{17}$ cm^{-2} implies $N(H_2)$=$3.3\ 10^{22}$

cm^{-2}, using $[^{13}CO]/[^{12}CO]$=60 and CO/H_2=2 10^{-4} based on Lacy et al. (1994). This would result in a $[H_2O]/[H_2]$ abundance of 6 10^{-5}, which is higher than the value of 10^{-5} inferred for several "hot core" regions from $H_2^{18}O$ submillimeter lines by Zmuidzinas et al. (1996) and Gensheimer et al. (1996). If both the 200 and 1000 K components contribute to the water spectrum this value decreases to 3 10^{-5}.

The question of the relative amount of H_2O in the warm and hot gas also relates directly to the physical environment. Gas at 1000 K must be close to the YSO if it is radiatively heated. At such high temperatures and densities, most of the oxygen not in CO is driven into H_2O. The only other mechanism would be through shocks associated with the outflow. It is well known that non–dissociative shock models give a high H_2O abundance of at least 10^{-4}, which would be comparable to or larger than the abundance seen here (e.g., Kaufman & Neufeld 1996). An argument against this mechanism is the presence of C_2H_2 in the same hot component, a molecule not easily accounted for by shocks (Carr et al. 1995). If H_2O resides primarily in the 200 K gas, it may be farther away from the YSO in the region where icy mantles evaporate from the grains and the mantle molecules contribute to a "hot core" chemistry (e.g., Millar et al. 1991; Charnley et al. 1992). Indeed, for GL 2591 the gas–phase H_2O abundance derived here is comparable to that of solid H_2O (see van Dishoeck & Helmich 1996).

Because of the low spectral resolution of the ISO data, we cannot fully exclude the presence of some H_2O in the broad, blue–shifted outflowing gas seen in CO absorption. However, the H_2 column density of this gas is at least a factor of 10 lower than that of the other components. If all of the H_2O were located in the outflowing gas, an abundance of 5 10^{-4} or higher would result, which could account for most of the oxygen abundance.

If the abundance of water is sufficiently high that it contains a large fraction of the gas–phase oxygen abundance, it can affect significantly the abundances of some species in a "hot core" model. Its major influence is a rapid rise of nitrogen–bearing molecules like HCN, HNC and CH_3CN. Since water is not very reactive, it hardly contributes to the chemistry itself. However, at high abundances it locks up a large fraction of atomic oxygen which is otherwise available for the destruction of small and complex organics. The rapid rise of the HCN abundance coupled with the constancy of the water abundance may serve as a sensitive chemical clock. The high observed abundance of HCN toward GL 2591 may be significant in this respect. Further studies are needed to investigate this possibility.

5. Conclusions

The detection of the bending mode of water toward AFGL 2591 with the ISO-SWS provides a new tool to study both the physical conditions and the water abundance in dense star–forming molecular clouds. The unique aspect of the infrared technique compared with emission line data is the observation of many ro-vibrational lines in the same spectrum. More detailed observations of H_2O and its isotopes with ISO and ground-based sub-millimeter telescopes are in progress. The comparison with ISO–LWS observations will be especially interesting, since many of the low–lying pure rotational lines should be excited in emission. High spectral resolution data are needed, however, to detect these lines on top of the strong continuum emission. Together these observations should provide a more complete view on the environment of this and other YSO's.

Acknowledgements. We are indebted to N.J. Evans, J.H. Lacy and G.A. Blake for many useful discussions concerning GL 2591. This work was supported by the Netherlands Organization for Scientific Research (NWO).

References

Blake, G.A., Mundy, L.G., Carlstrom, J.E., et al., 1996, ApJ in press
Camy–Peyret, C., Flaud, J.–M., 1976, Molec. Phys. 32, 532
Carr, J.S., Evans, N.J., Lacy, J.H., Zhou, S., 1995, ApJ 450, 667
Cernicharo, J., Thum, C., Hein, H., et al., 1990, A&A 231, L15
Cernicharo, J., González-Alfonso, E., Alcolea, J., et al., 1994, ApJ 432, L59
Charnley, S.B., Tielens, A.G.G.M., Millar, T.J., 1992, ApJ 399, L71
Cheung, A.C., Rank, D.M., Townes, C.H., et al., 1969, Nature 221, 626
de Graauw, Th. et al., 1996, A&A this volume
Geballe, T.R., Wade, R., 1985, ApJ 291, L55
Gensheimer, P., Mauersberger, R., Wilson, T.L., 1996, A&A in press
Green, S., Maluendes, S., McLean, A.D. 1993, ApJS 85, 181
Helmich, F.P., 1996, PhD thesis University of Leiden
Jacq, T., Jewell, P.R., Henkel, C., et al., 1988, A&A 199, L5
Kaufman, M.J., Neufeld, D.A., 1996, ApJ 456, 611
Kessler, M.F. et al., 1996, A&A this volume
Knacke, R.F., Larson, H.P., Noll, K.S., 1988, ApJ 335, L27
Knacke, R.F., Larson, H.P., 1991, ApJ 367, 162
Lacy, J.H., Baas, F., Allamandola, L.J., et al., 1984, ApJ 276, 533
Lacy, J.H., Knacke, R., Geballe, T.R., Tokunaga, A.T., 1994, ApJ 428, L69
Melnick, G.J., Menten, K.M., Phillips, T.G., Hunter, T., 1993, ApJ 416, L37
Millar, T.J., Herbst, E., Charnley, S.B., 1991, ApJ 369, 147
Mitchell, G.F., Curry, C., Maillard, J.-P., Allen, M., 1989, ApJ 341, 1020
Mitchell, G.F., Maillard, J.-P., Allen, et al., 1990, ApJ 363, 554
Neufeld, D.A., Melnick, G.J., 1991, ApJ 368, 215
Phillips, T.G., Kwan, J., Huggins, P.J., 1980, in: IAU Symp. 87, Interstellar Molecules, ed. B.H. Andrew, Reidel, Dordrecht, 21
Rothman, L.S., Gamache, R.R., Tipping, R.H. et al., 1992, J. Quant. Spectrosc. Radiat. Transfer, 48, 537
Schaeidt, S.G., et al., 1996, A&A this volume
Tauber, J., Olofsson, G., Pilbratt, G., Nordh, L., Frisk, U., 1996, A&A 308, 913
Tofani, G., Felli, M., Taylor, G.B., Hunter, T.R., 1995, A&AS 112, 299
Valentijn, E.A. et al., 1996, A&A this volume
van Dishoeck, E.F., Helmich, F.P., 1996, A&A this volume
van Dishoeck, E.F., et al., 1996, A&A this volume
Wannier, P.G., Pagani, L., Kuiper, T.B.H., et al., 1991, ApJ 377, 171
Waters, J.W., Gustincic, J.J., Kakar, R.K. et al., 1980, ApJ 235, 57
Zmuidzinas, J., Blake, G.A., Carlstrom, J., et al., 1996, ApJ, submitted